J|A|C|S
ARTICLES

Published on Web 05/04/2009

Noncovalently Netted, Photoconductive Sheets with Extremely High Carrier Mobility and Conduction Anisotropy from Triphenylene-Fused Metal Trigon Conjugates

Long Chen,[†] Jangbae Kim,[‡] Tomoya Ishizuka,[†] Yoshihito Honsho,[§] Akinori Saeki,[§] Shu Seki,*[,§] Hyotcherl Ihee,*[,‡] and Donglin Jiang*[,†]

Department of Materials Molecular Science, Institute for Molecular Science and PRESTO, JST, 5-1 Higashiyama, Myodaiji, Okazaki 444-8787, Japan, Center for Time-Resolved Diffraction, Department of Chemistry, KAIST, Daejeon 305-701, Republic of Korea, and Department of Applied Chemistry, Graduate School of Engineering, Osaka University and PRESTO, JST, 2-1 Yamadaoka, Suita, Osaka 565-0871, Japan

Received February 27, 2009; E-mail: hyotcherl.ihee@kaist.ac.kr; seki@chem.eng.osaka-u.ac.jp; jiang@ims.ac.jp

Abstract: Supramolecular assembly of small molecules via noncovalent interaction is useful for bottom-up construction of well-defined macroscopic structures. This approach is attracting increasing interest due to its high potential in manufacturing novel molecular electronic and optoelectronic devices. This Article describes the synthesis and functions of a sheet-shaped assembly from novel triphenylene-fused metal trigon conjugates. These conjugates were recently designed and synthesized by a divergent method and used for the supramolecular self-assembly of sheet-like objects. In contrast to triphenylene, which absorbs photons in ultraviolet region, the triphenylene-fused metal trigon conjugate shows a strong absorption band in the visible region. The metal trigon conjugate emits green photoluminescence with significantly enhanced quantum yield and allows intramolecular energy migration, as a result of extended π-conjugation over metal sites. It assembles via physical gelation to form noncovalent sheets that collect a wide wavelength range of photons from ultraviolet to visible regions. The noncovalent sheets allow exciton migration and are semiconducting with an extremely large intrinsic carrier mobility of 3.3 $cm^2\ V^{-1}\ s^{-1}$. They are highly photoconductive, produce photocurrent with a quick response to light irradiation, and are capable of repetitive on−off switching. Moreover, these sheets facilitate a conduction path perpendicular to the sheet plane, thus exhibiting a spatially distinctive anisotropy in conduction. The noncovalent sheet assemblies with these unique characteristics are important for molecular optoelectronic devices based on solution-processed soft materials.

Introduction

Conjugated molecules have been a central subject of studies in the fields of organic electronics and optoelectronics.[1] Introduction of metal modules to conjugated molecules plays an important role in expanding the diversity of supramolecular self-assembly. For example, the properties of metal ions such as magnetism, and redox and photochemical activities, may be transcribed on the supramolecules. In this context, triphenylene, a typical conjugated planar molecule, is an intriguing motif for this purpose because of its utility in supramolecular assembly.[2−4] However, to date, metal-containing triphenylene derivatives have been limited to thio-ligated bismuth[5a] and silver[5b] crystalline solids. Here, we report the first example of triphenylene-fused metal trigon conjugates (Chart 1; **TSZn$_3$**), where multinuclear metal sites[6] are connected to one another via conjugation with a triphenylene core. **TSZn$_3$** emits green photoluminescence with a significantly enhanced quantum yield and allows intramolecular energy migration between metal sites as a result of

[†] Institute for Molecular Science.
[‡] KAIST.
[§] Osaka University.

(1) (a) Brunsveld, L.; Folmer, B. J. B.; Meijer, E. W.; Sijbesma, R. P. *Chem. Rev.* **2001**, *101*, 4071–4097. (b) Bong, D. T.; Clark, T. D.; Granja, J. R.; Ghadiri, M. R. *Angew. Chem., Int. Ed.* **2001**, *40*, 988–1011. (c) Schmidt-Mende, L.; Fechtenkotter, A.; Müllen, K.; Moons, E.; Friend, R. H.; MacKenzie, J. D. *Science* **2001**, *293*, 1119–1122. (d) Hoeben, F. J. M.; Jonkheijm, P.; Meijer, E. W.; Schenning, A. P. H. J. *Chem. Rev.* **2005**, *105*, 1491–1546. (e) Hameren, R. V.; Schn, P.; Buul, A. M. V.; Hoogboom, J.; Lazarenko, S. V.; Gerritsen, J. W.; Engelkamp, H.; Christianen, P. C. M.; Heus, H. A.; Maan, J. C.; Rasing, T.; Speller, S.; Rowan, A. E.; Elemans, J. A. A. W.; Nolte, R. J. M. *Science* **2006**, *314*, 1433–1436. (f) Hill, J. P.; Jin, W.; Kosaka, A.; Fukushima, T.; Ichihara, H.; Shimomura, T.; Ito, K.; Hashizume, T.; Ishii, N.; Aida, T. *Science* **2004**, *304*, 1481–1483. (g) Palmer, L. C.; Stupp, S. I. *Acc. Chem. Res.* **2008**, *41*, 1674–1684. (h) Klok, H. A.; Joliffe, K. A.; Schauer, C. L.; Prins, L. J.; Spatz, J. P.; Möller, M.; Timmerman, P.; Reinhoudt, D. N. *J. Am. Chem. Soc.* **1999**, *121*, 7154–7155.

(2) (a) Shen, Z.; Yamada, M.; Miyake, M. *J. Am. Chem. Soc.* **2007**, *129*, 14271–14280. (b) Cui, L.; Collet, J. P.; Xu, G.; Zhu, L. *Chem. Mater.* **2006**, *18*, 3503–3512. (c) Duzhko, V.; Shi, H.; Singer, K. D.; Semyonov, A. N.; Twieg, R. J. *Langmuir* **2006**, *22*, 7947–7951.

(3) Selected reviews: (a) Laschat, S.; Baro, A.; Steinke, N.; Giesselmann, F.; Hägele, C.; Scalia, G.; Judele, R.; Kapatsina, E.; Sauer, S.; Schreivogel, A.; Tosoni, M. *Angew. Chem., Int. Ed.* **2007**, *46*, 4832–4887. (b) Kumar, S. *Liq. Cryst.* **2004**, *31*, 1037–1059. (c) Kumar, S. *Liq. Cryst.* **2005**, *32*, 1089–1113. (d) Sergeyev, S.; Pisula, W.; Geerts, Y. H. *Chem. Soc. Rev.* **2007**, *36*, 1902–1929.

Chart 1. (a) Schematic Representation of Triphenylene-Fused Trigons **TSH$_6$** and **TSZn$_3$**, Nonalkoxylated Trigon, and Their Controls **SH$_2$** and **SZn**; and (b) Lattice Packing of the Assembled 2D Sheets

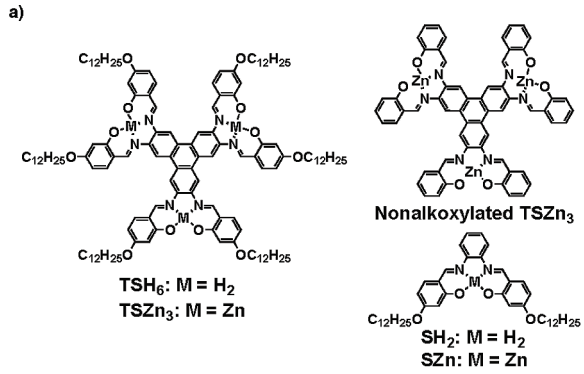

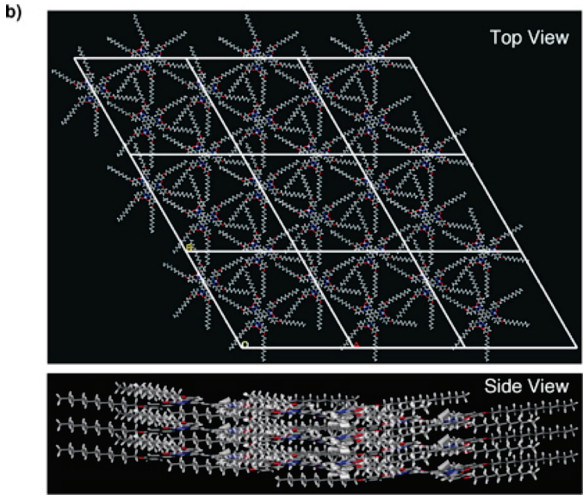

extended π-conjugation. In contrast to the 1D arrays reported for triphenylene derivatives,[2,3] self-assembly of **TSZn$_3$** leads to the construction of a 2D sheet. We found that the assembled 2D sheet collects photons over a wide wavelength range from the ultraviolet to visible regions, converts them to bright luminescence, and allows exciton migration. Furthermore, the noncovalent 2D sheet is electrically semiconducting and capable of repetitive on−off switching. The 2D sheet shows photoconductivity with a quick response to the irradiation of a wide range of visible light with a large on/off ratio. A clear spatial anisotropy reveals that the sheet assembly favors a conduction path perpendicular to the stacked sheets rather than that along the sheet plane.

Experimental Section

THF was distilled over benzophenone ketyl under Ar before use. Other organic solvents for reactions were distilled over the appropriate drying reagents under argon or obtained as dehydrated reagents from Kanto Chemicals. Tris(dibenzylideneacetone)dipalladium(0), sodium *tert*-butoxide, and *rac*-BINAP were obtained from Tokyo Kasei Co. (TCI). Zinc(II) acetate dihydrate was obtained from Kanto Chemicals. Benzophenone imine and triethylamine were obtained from Aldrich. Wakogel C-300HG was used for column chromatography. Deuterated solvents for NMR measurement were obtained from Cambridge Isotope Laboratories, Inc. Solvents for gelation test were spectroscopic grade and used as received.

Results and Discussion

TSZn$_3$ was synthesized by metalation of **TSH$_6$** with zinc(II) acetate and unambiguously characterized by various spectroscopies (see Supporting Information). A divergent method was developed for the synthesis of the unprecedented **TSH$_6$** from triphenylene. Electronic absorption spectroscopy revealed an extended π-electronic conjugation in the triphenylene-fused trigons. As indicated by the blue curve in Figure 1, **TSH$_6$** in CH_2Cl_2 at 23 °C exhibits an absorption band due to the $\pi-\pi^*$ transition at 379 nm, which is red-shifted by 94 and 48 nm from those of triphenylene (285 nm; black curve) and a mono-Schiff-base control **SH$_2$** (331 nm; dotted blue curve), respectively. In relation to this observation, **TSZn$_3$** exhibits an absorption band at 419 nm (red curve) and a 44 nm red-shift from the mononuclear reference **SZn** (375 nm; dotted red curve).[7] As all of the above samples are highly soluble in CH_2Cl_2, we thus evaluated the absorption coefficients by plotting absorbance versus concentrations, which gives a good linear

(4) Triphenylene-based liquid crystalline. Müllen's group: (a) Yatabe, T.; Harbison, M. A.; Brand, J. D.; Wagner, M.; Müllen, K.; Samori, P.; Rabe, J. P. *J. Mater. Chem.* **2000**, *10*, 1519–1525. (b) Miskiewice, P.; Rybak, A.; Jung, J.; Glowacki, I.; Ulanski, J.; Geerts, Y.; Watson, M.; Müllen, K. *Synth. Met.* **2003**, *137*, 905–906. Geerts's group: (c) Rybak, A.; Pfleger, J.; Jung, J.; Pavlik, M.; Glowacki, I.; Ulanski, J.; Tomovic, Z.; Mullen, K.; Geerts, Y. H. *Synth. Met.* **2006**, *156*, 302–309. (d) Lehmann, M.; Kestemont, G.; Aspe, R. G.; Buess-Herman, C.; Koch, M. H. J.; Debije, M. G.; Piris, J.; de Haas, M. P.; Warman, J. M.; Watson, M. D.; Lemaur, V.; Cornil, J.; Geerts, Y. H.; Gearba, R.; Ivanov, D. A. *Chem.-Eur. J.* **2005**, *11*, 3349–3362. (e) Lemaur, V.; da Silva Filho, D. A.; Coropceanu, V.; Lehmann, M.; Geerts, Y.; Piris, J.; Debije, M. G.; van de Craats, A. M.; Senthikumar, K.; Siebbeles, L. D. A.; Warman, J. M.; Bredas, J.-L.; Cornil, J. *J. Am. Chem. Soc.* **2004**, *126*, 3271–3279. (f) Kestemont, G.; de Halleux, V.; Lehmann, M.; Ivanov, D. A.; Watson, M.; Geerts, Y. H. *Chem. Commun.* **2001**, 2074–2075. Preece's group: (g) Donovan, K. J.; Scott, K.; Somerton, M.; Preece, J.; Manickam, M. *Chem. Phys.* **2006**, *322*, 471–476. (h) Manickam, M.; Cooke, G.; Kumar, S.; Ashton, P. R.; Preece, J.; Spencer, N. *Mol. Cryst. Liq. Cryst.* **2003**, *397*, 399–416. (i) Manickam, M.; Belloni, M.; Kumar, S.; Varshney, S. K.; Shankar Rao, D. S.; Ashton, P. R.; Preece, J.; Spencer, N. *J. Mater. Chem.* **2001**, *11*, 2790–2800. (j) Allen, M. T.; Diele, S.; Harris, K. D. M.; Hegmann, T.; Kariuki, B. M.; Lose, D.; Preece, J.; Tschierske, C. *J. Mater. Chem.* **2001**, *11*, 302–311. Bushby's group: (k) Holt, L. A.; Bushby, R. J.; Evans, S. D.; Burgess, A.; Seeley, G. *J. Appl. Phys.* **2008**, *103*, 063712. (l) Lino, H.; Hanna, J.-i.; Bushby, R. J.; Movaghar, B.; Whitaker, B. J. *J. Appl. Phys.* **2006**, *100*, 043716. (m) Lino, H.; Hanna, J.-i.; Bushby, R. J.; Movaghar, B.; Whitaker, B. J.; Cook, M. J. *Appl. Phys. Lett.* **2005**, *87*, 132102. (n) Bushby, R. J.; Lozman, O. R. *Curr. Opin. Solid State Mater. Sci.* **2003**, *6*, 569–578. (o) Wegewijs, B. R.; Siebbeles, L. D. A.; Boden, N.; Bushby, R. J.; Movaghar, B.; Lozman, O. R.; Liu, Q.; Pecchia, A.; Mason, L. A. *Phys. Rev. B: Condens. Matter* **2002**, *65*, 245112. (p) Hughes, R. E.; Hart, S. P.; Smith, D. A.; Movaghar, B.; Bushby, R. J.; Boden, N. *J. Phys. Chem. B* **2002**, *106*, 6638–6645. (q) Pecchia, A.; Lozman, O. R.; Movaghar, B.; Boden, N.; Bushby, R. J.; Donovan, K. J.; Kreouzis, T. *Phys. Rev. B: Condens. Matter* **2002**, *65*, 104204. (r) Bushby, R. J.; Evans, S. D.; Lozman, O. R.; McNeill, A.; Movaghar, B. *J. Mater. Chem.* **2001**, *11*, 1982–1984.

(5) (a) Xu, Z.; Li, K.; Fettinger, J. C.; Li, J.; Michael, M. A. *Cryst. Growth Des.* **2005**, *5*, 423–425. (b) Li, K.; Xu, Z.; Xu, H.; Carroll, P. J.; Fettinger, J. C. *Inorg. Chem.* **2006**, *45*, 1032–1037.

(6) Reported trisalphen metal complexes: (a) Glaser, T.; Heidemeier, M.; Strautmann, J. B. H.; Bögge, H.; Stammler, A.; Krickemeyer, E.; Huenerbein, R.; Grimme, S.; Bothe, E.; Bill, E. *Chem.-Eur. J.* **2007**, *13*, 9191–9206. (b) Ma, C. T. L.; MacLachlan, M. J. *Angew. Chem., Int. Ed.* **2005**, *44*, 4178–4182. (c) Glaser, T.; Heidemeier, M.; Frohlich, R.; Hildebrandt, P.; Bothe, E.; Bill, E. *Inorg. Chem.* **2005**, *44*, 5467–5482. (d) Ma, C.; Lo, A.; Abdolmaleki, A.; MacLachlan, M. J. *Org. Lett.* **2004**, *6*, 3841–3844.

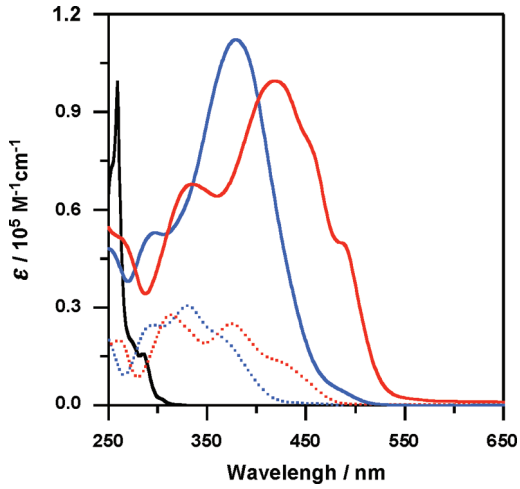

Figure 1. Electronic absorption spectra of **TSH$_6$** (blue curve) and **TSZn$_3$** (red curve) as compared to that of triphenylene (black curve), and control compounds **SH$_2$** (dotted blue curve) and **SZn** (dotted red curve), in CH_2Cl_2 at 25 °C (8.9×10^{-6} M; at this concentration no aggregation occurs).

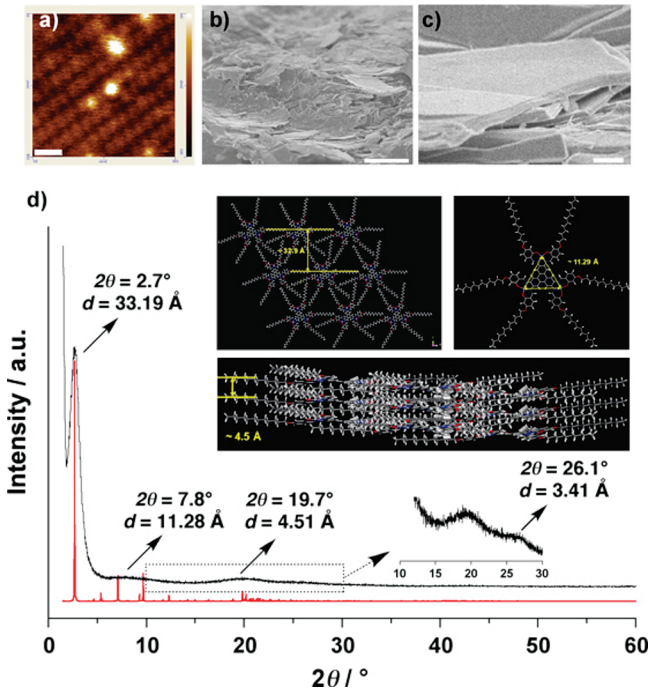

Figure 2. (a) STM image of **TSZn$_3$** on an HOPG substrate (bar: 10 nm). (b) Large-area FE-SEM image of xerogel of **TSZn$_3$** (bar: 10 μm). (c) A high magnification image of layered sheets (bar: 500 nm). (d) Experimental (black curve) and simulated (red curve) PXRD patterns of the sheet and simulated molecular packing structure (insets). The enlarged PXRD curve shows a broad and weak peak at $2\theta = 26.1°$, corresponding to a d value of 3.41 Å, which is reasonable for $\pi-\pi$ stacking.

correlation (Figure S2). These results indicate that conjugation is extended from the focal triphenylene core to the mounted metal sites. Consequently, **TSH$_6$** and **TSZn$_3$** display significantly expanded light absorption windows along with largely enhanced absorption coefficients (Figure 1; 8.9×10^{-6} M).

TSZn$_3$ formed a well-defined sheet-shaped monolayer on an HOPG substrate by casting a $CHCl_3$ solution, as revealed by STM (Figure 2a). In a hydrocarbon solvent such as decalin, **TSZn$_3$** self-assembles to form a physical gel (Figure S3; Table S1).[8,9] When added to decalin, **TSZn$_3$** gradually dissolved upon heating at 80 °C to produce a dark red solution (9.0 mM, 20 mg/mL). When the solution was allowed to stand at 25 °C for 5 min, it formed a red-orange physical gel. On heating at 70 °C, the gel of **TSZn$_3$** became fluid and eventually turned into a solution, and the gel-to-sol transition temperature was estimated to be 48 °C (Figures S3 and S4).[9a] The sol−gel transition is thermally reversible many times. FE-SEM images of a freeze-dried xerogel reveal that it consists of 2D sheets without any other morphologies such as spheres, fibers, ribbons, or rods (Figure 2b). One-by-one examination of the objects shows that the sheets are extended two-dimensionally for several micrometers in length and width (Figure 2c), while the thickness varies from a few nanometers to several hundred nanometers, as identified by AFM measurement. Reports of noncovalent sheet assembly are rarely in the literature,[10] while other textures such as spheres, fibers, rods, ribbons, and tubes have been well developed in supramolecular systems. Although PXRD measurement of the xerogel exhibits broad peaks in the wide angle range, reflections at 2.7°, 8.6°, 19.7°, and 26.1° (Figure 2d; black curve) can be identified. To elucidate the molecular packing, we first conducted quantum chemical calculation at the AM1 level performed on Spartan'04 (Wave function, Inc.) to optimize the **TSZn$_3$** geometry, and then performed molecular modeling and Pawley refinement by using Reflex, implemented in the Materials Studio program package version 4.3.[11] Simulation using the $P32$ space group (No. 145) with $a = b = 65.8262$ Å and $c = 4.4916$ Å results in a PXRD pattern (Figure 2d; red curve) that is in good agreement with that observed experimentally. All of the diffractions can be reasonably assigned. Therefore, **TSZn$_3$** most likely assembles in a trigonal manner with interdigitated alkyl chains to form 2D sheets that stack to afford a layered structure (Figure 2d; Chart 1b; Figures S5−S7).

The molecular ordering in the sheet assembly is morphologically similar to the lattice structure of single crystals of a triphenylene-fused Zn(II) trigon without alkyl chains (Figure

(7) Di Bella, S.; Fragalà, I.; Ledoux, I.; Diaz-Garcia, M. A.; Marks, T. J. *J. Am. Chem. Soc.* **1997**, *119*, 9550–9557.
(8) Selected reviews on gels containing metal species: (a) Fages, F. *Angew. Chem., Int. Ed.* **2006**, *45*, 1680–1682. (b) Kato, T.; Hirai, Y.; Nakaso, S.; Moriyama, M. *Chem. Soc. Rev.* **2007**, *36*, 1857–1867. (c) Leininger, S.; Olenyuk, B.; Stang, P. J. *Chem. Rev.* **2000**, *100*, 853–908. (d) Dobrawa, R.; Würthner, F. *J. Polym. Sci., Part A: Polym. Chem.* **2005**, *43*, 4981–4995.
(9) Selected papers on gels containing metal species: (a) Tu, T.; Bao, X.; Assenmacher, W.; Peterlik, H.; Danies, J.; Dötz, K. H. *Chem.-Eur. J.* **2009**, *15*, 1853–1861. (b) Tu, T.; Assenmacher, W.; Peterlik, H.; Weisbarth, R.; Nieger, M.; Dötz, K. H. *Angew. Chem., Int. Ed.* **2007**, *46*, 6368–6371. (c) Bühler, G.; Feiters, M. C.; Nolte, R. J. M.; Dötz, K. H. *Angew. Chem., Int. Ed.* **2003**, *42*, 2494–2497. (d) Klawonn, T.; Gansäuer, A.; Winkler, I.; Lauterbach, T.; Franke, D.; Nolte, R. J. M.; Feiters, M. C.; Börner, H.; Hentschel, J.; Dötz, K. H. *Chem. Commun.* **2007**, 1894–1895. (e) Beck, J. B.; Rowan, S. J. *J. Am. Chem. Soc.* **2003**, *125*, 13922–13923. (f) Ishi-i, T.; Iguchi, R.; Snip, E.; Ikeda, M.; Shinkai, S. *Langmuir* **2001**, *17*, 5825–5833. (g) Shirakawa, M.; Kawano, S.; Fujita, N.; Sada, K.; Shinkai, S. *J. Org. Chem.* **2003**, *68*, 5037–5044. (h) Kimura, M.; Muto, T.; Takimoto, H.; Shirakawa, K. M.; Fujita, N.; Tani, T.; Kaneko, K.; Shinkai, S. *Chem. Commun.* **2005**, 4149–4151. (i) Kawano, S.-i.; Fujita, N.; Shinkai, S. *J. Am. Chem. Soc.* **2004**, *126*, 8592–8593. (j) Kishimura, A.; Yamashita, T.; Aida, T. *J. Am. Chem. Soc.* **2005**, *127*, 179–183. (k) Kishimura, A.; Yamashita, T.; Yamaguchi, K.; Aida, T. *Nat. Mater.* **2005**, *4*, 546–549. (l) Hui, J. K.-H.; Yu, Z.; MacLachlan, M. J. *Angew. Chem., Int. Ed.* **2007**, *46*, 7980–7983.
(10) Mukhopadhyay, P.; Iwashita, Y.; Shirakawa, M.; Kawano, S.; Fujita, N.; Shinkai, S. *Angew. Chem., Int. Ed.* **2006**, *45*, 1592–1595.
(11) Accelrys, Material Studio Release Notes, Release 4.3, Accelrys Software, San Diego, CA, 2008.

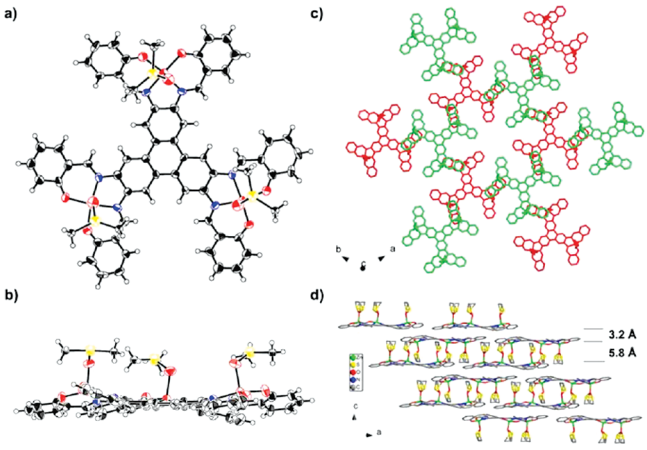

Figure 3. Crystal structure of nonalkoxylated **TSZn$_3$**. (a) Top and (b) side views of one molecule. (c) Top and (d) and side views of crystal packing. DMSO solvent coordinates with each Zn(II).

3).[12] The triphenylene-fused trigon is almost planar (Figure 3a and b). Each Zn(II) atom is five-coordinated with four equatorial sites occupied by two salicylidene−imine units and one axial site by an oxygen atom from a coordinated DMSO molecule (Figure 3a). As shown in Figure 3c, within one bilayer (the trigons in red are in the same sheet, while the neighboring sheet in green is staggered over the red one), each molecule is stacked with three molecules of the neighboring sheet through $\pi-\pi$ interaction ($\pi-\pi$ distance = 3.24 Å). The bilayer further stacks in the c direction to form a layered sheet structure, where the interbilayer distance is 5.79 Å and between the bilayers are located the axial and non-coordinating DMSO molecules (Figure 3d).

The photochemical properties of **TSZn$_3$** both in the solution and during assembly were studied in comparison with a control **SZn**. Upon excitation at 390 nm in CH_2Cl_2 at 25 °C, **SZn** emits a weak fluorescence at 484 nm (Figure 4a; blue curve) with a quantum yield (Φ_{FL}) of only 0.3%. In sharp contrast, **TSZn$_3$** emits green fluorescence at 503 and 535 nm (green curve) with a Φ_{FL} value of 11.5%, which is almost 30-fold that of **SZn**. On the other hand, when excited with light ranging from 250 to 500 nm, the gel produces similar luminescence at 570 and 606 nm (red curve). The Φ_{FL} value of the gel was estimated to be 7%. The large red-shifted emission with an enhanced quantum yield is clearly the result of extended π-conjugation and $\pi-\pi$ stacking interaction.[13] These observations indicate that the 2D sheets can absorb photons over a wide wavelength range from ultraviolet to visible regions and convert them to bright green-orange emission.

Because extended π-electronic conjugation is present, we assumed that excitation energy would migrate over the trigon conjugates. Thus, the fluorescence depolarization characteristics of **TSZn$_3$** were investigated upon excitation with polarized light

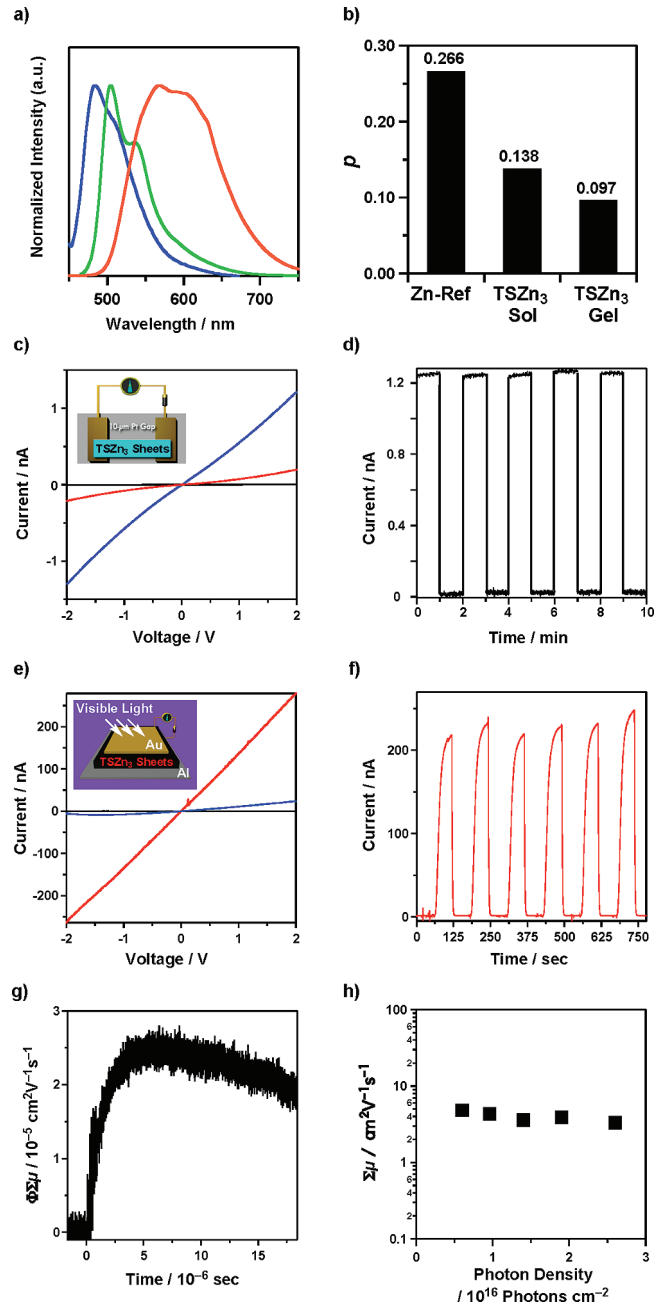

Figure 4. (a) Normalized fluorescence spectra of **SZn** (blue curve), **TSZn$_3$** in CH_2Cl_2 (green curve), and **TSZn$_3$** gel (red curve). (b) Fluorescence depolarization profile. (c) $I-V$ profile of a 10 μm-wide Pt gap (black curve, without a **TSZn$_3$** sheet; red curve, with a **TSZn$_3$** sheet; blue curve, with an iodine-doped **TSZn$_3$** sheet). (d) Electric current when a 2 V bias voltage is turned on or off. (e) $I-V$ profile of a **TSZn$_3$** sheet sandwiched between Al/Au electrodes (blue curve, without light irradiation; red curve, upon visible light irradiation). (f) Photocurrent when light is turned on or off. (g) FP TRMC profile of the **TSZn$_3$** sheet at 25 °C on irradiation with a 355 nm pulse laser at a power of 2.6×10^{16} photons cm^{-2}. (h) Dependence of minimum mobility of the charge carrier of the **TSZn$_3$** sheet on photon density (local carrier density).

in a viscous medium such as polyethylene glycol (PEG).[14] **SZn** exhibits the highest retentivity in fluorescence depolarization (Figure 4b; p = 0.266). The fluorescence of **TSZn$_3$** was considerably depolarized to result in a decreased p value (0.138), indicating that the excitation energy most likely migrates over the nanosized trigon. Of interest, **TSZn$_3$** gel exhibits more significant depolarization in fluorescence to afford the lowest p

(12) Crystal data for the non-alkoxylated triphenylene-fused Zn trigon, $C_{60}H_{36}N_6O_6Zn_3 \cdot 11C_2H_6OS$: trigonal, space group R-3(h) (No. 148), $a = b = 24.94(3)$, $c = 26.91(4)$ Å. $\alpha = \beta = 90°$, $\gamma = 120°$, $V = 14501(32)$ Å^3. $Z = 6$, final $R_1 = 0.137$ ($I > 2\sigma(I)$), w$R_2 = 0.480$ (all the reflections), and GOF = 1.133. The refinement was based on 7360 independent reflections out of total 7360 reflections collected and 368 variable parameters. Crystallographic data have been deposited at the Cambridge Crystallographic Data Centre with reference number CCDC 675626.

(13) Yamaguchi, Y.; Matsubara, Y.; Ochi, T.; Wakamiya, T.; Yoshida, Z.-i. *J. Am. Chem. Soc.* **2008**, *130*, 13867–13869.

value of only 0.097. Therefore, the excitation energy is not localized but can migrate over the sheets. Such an exciton migration is highly interesting from the viewpoint of developing molecular optoelectronics.

Single crystals of triphenylene have been reported to function as semiconductors.[15] The well-defined molecular order of the assembled 2D sheets indicates a high probability of becoming electrically semiconducting. We investigated this possibility by measuring the electrical conductivity across a 10 μm-wide Pt gap by a two-probe method (Figure 4c; inset). The 2D sheet shows an almost linear $I-V$ profile in air at 25 °C (Figure 4c; red curve), while the gap itself is unresponsive (black curve) irrespective of bias voltage. For example, at a 2 V bias voltage, the sheet shows an electric current of 0.25 nA. The unassembled sample (as-synthesized) of **TSZn$_3$**, however, exhibits a low current (Figure S8a; 20 pA) under otherwise identical conditions. This is also the case for **SZn** (Figure S8b; 8 pA). Thus, the high conductivity observed for **TSZn$_3$** is clearly related to the highly ordered alignment of the conjugated metal trigon. Doping with iodine (Figure S9)[16] increased the electric current (Figure 4c; blue curve), suggesting that the self-assembled 2D sheet is a p-type semiconductor. Furthermore, the current can be switched on−off repetitively without significant deterioration (Figure 4d). Cyclic voltammetry of **TSZn$_3$** reveals that the first oxidation potential is as low as 0.28 V vs Fc^+/Fc (Figure S10), suggesting a facile generation of charge carriers with an oxidative dopant such as iodine.[17]

Along this line, we further investigated the light irradiation effect on the conductivity of the 2D sheets, because triphenylene single crystal has been reported to be photoconductive on irradiation with ultraviolet light, as a result of exciton migration followed by charge separation at the molecule−electrode interface.[18] Accordingly, we sandwiched the 2D sheets between Al/Au electrodes to examine this possibility (Figure 4e, inset). Upon irradiation with visible light (>400 nm), the 2D sheets show an almost linear $I-V$ profile with significantly enhanced current (Figure 4e; red curve). In contrast to the sheet of **TSZn$_3$**, triphenylene lacks an absorption window in the visible region (Figure 1; black curve); thus, it barely responds to visible light irradiation. On−off experiments revealed that the photocurrent shows a quick response to light irradiation and can be repetitively switched many times with an on−off ratio of about 200 (Figure 4f). In contrast, the 2D sheets bridged on the Pt gap electrodes show photocurrent generation but with a low current increment and a low on−off ratio of only 30 (Figure S11). Such spatial anisotropy in photocurrent generation suggests that a conduction path perpendicular to the stacked sheets is superior to that along the sheet plane.

To evaluate the intrinsic carrier mobility, we conducted laser flash photolysis time-resolved microwave conductivity measurements (FP TRMC; see Supporting Information).[19] The transient conductivity profile shows a rapid rise upon laser irradiation, to yield a $\Phi\Sigma\mu$ value of 2.8×10^{-5} cm^2 V^{-1} s^{-1} at a photon density of 2.6×10^{16} photons/cm^2 (Figure 4g). To determine the number of charge carriers, time-of-flight transient was integrated at different bias voltages (Figures S12 and S13). The number of charge carriers estimated by extrapolation of the bias at 0 V was 1.8×10^8, leading to the charge carrier generation yield (Φ; number of charge carrier/number of photon) of 8.5×10^{-6}. Therefore, the minimum carrier mobility ($\Sigma\mu$) was evaluated to be 3.3 cm^2 V^{-1} s^{-1}. It is noted that the carrier mobility is maintained almost constant when different photon densities are applied (Figure 4h), suggesting that free charge carriers are generated by single photon processes via the trigon excited states. The relatively slow rise-time of the conductivity transient ($k = 3 \times 10^5$ s^{-1}) also supports the charge carriers produced by migrated excitons rather than the singlet excited state of single molecule. The intrinsic carrier mobility is extremely high as compared to small organic semiconductors,[20] conjugated polymers[21] including the state-of-the-art semiconducting polymer, *RR*-P3HT ($\mu = 0.014$ cm^2 V^{-1} s^{-1}),[22] and liquid crystalline system,[23] and is most likely related to the highly ordered molecular structure in the sheet assembly.

Conclusions

Exploration of metal-ion integrated conjugation systems has a high probability of leading to the development of new materials. In summary, we reported an unprecedented π-conjugation system with electronically correlated multinuclear metal sites on a fused triphenylene trigon. Upon self-assembly, the metal trigon forms a well-defined 2D sheet, which harvests a wide range of photons, converts them to bright emission, and allows exciton migration. Moreover, the 2D sheet is semiconducting, shows an extremely high carrier mobility, and is capable of repetitive on−off current switching at room temperature. The noncovalent 2D sheet is photoconductive and exhibits a quick response to visible light irradiation with a large on/off ratio and a significant spatial anisotropy. These characteristics are unique and clearly originate from the highly ordered molecular structure of the noncovalent sheet assembly, thus casting a sharp contrast to the triphenylene precursor. Therefore, the multifunctional sheets constitute an important step for molecular optoelectronics based on soft materials.

(14) When a chromophore with a restricted Brownian motion is excited by polarized light, it emits a polarized fluorescence. However, the fluorescence should be depolarized when the excitation energy migrates randomly within the lifetime of the excited state. Here, fluorescence anisotropy (p) is defined by $(I_{||} - GI_{\perp})/(I_{||} + GI_{\perp})$, where $I_{||}$ and $I_{\perp}$ are fluorescence intensities of parallel and perpendicular components relative to the polarity of the excitation light, respectively, while G is an instrumental correction factor.

(15) (a) Santoro, A. V.; Mickevicius, G. *Chem. Phys. Lett.* **1975**, *36*, 658–660. (b) Vaughan, G. B. M.; Heiney, P. A.; McCauley, J. P., Jr.; Smith, A. B. *Phys. Rev. B* **1992**, *46*, 2787–2791.

(16) IR and electronic absorption spectroscopies were utilized for the characterization of iodine doping. A charge-transfer band at 1023 cm^{-1} was newly observed for the xerogel of **TSZn$_3$** upon exposure to iodine vapors (Figure S9a). Moreover, electronic absorption spectroscopy shows that exposure to iodine vapors induces a clear blue shift of the absorption band from 415 to 382 nm (Figure S9b), which is characteristic of complex formation between a triphenylene derivative and iodine, as reported in ref 15a.

(17) Puigmartí-Luis, J.; Laukhin, V.; Pérez del Pino, Á.; Vidal-Gancedo, J.; Rovira, C.; Laukhina, E.; Amabilino, D. B. *Angew. Chem., Int. Ed.* **2007**, *46*, 238–241.

(18) Almeleh, N.; Harrison, S. E. *J. Phys. Chem. Solids* **1965**, *26*, 1571–1584.

(19) Acharya, A.; Seki, S.; Koizumi, Y.; Saeki, A.; Tagawa, S. *J. Phys. Chem. B* **2005**, *109*, 20174–20179.

(20) Amaya, T.; Seki, S.; Moriuchi, T.; Nakamoto, K.; Nakata, T.; Sakane, H.; Saeki, A.; Tagawa, S.; Hirao, T. *J. Am. Chem. Soc.* **2009**, *131*, 408–409.

(21) Saeki, A.; Ohsaki, S.-i.; Seki, S.; Tagawa, S. *J. Phys. Chem. C* **2008**, *112*, 16643–16650.

(22) (a) Yamagami, R.; Kobayashi, K.; Saeki, A.; Seki, S.; Tagawa, S. *J. Am. Chem. Soc.* **2006**, *128*, 2212–2213. (b) Dicker, G.; de Haas, M. P.; Warman, J. M.; de Leeuw, D. M.; Siebbeles, L. D. A. *J. Phys. Chem. B* **2004**, *108*, 17818–17824. (c) Dicker, G.; de Haas, M. P.; Siebbeles, L. D. A.; Warman, J. M. *Phys. Rev. B* **2004**, *70*, 045203.

(23) Li, W.-S.; Yamamoto, Y.; Fukushima, T.; Saeki, A.; Seki, S.; Tagawa, S.; Masunaga, H.; Sasaki, S.; Takata, M.; Aida, T. *J. Am. Chem. Soc.* **2008**, *130*, 8886–8887.

Acknowledgment. This work was supported by Precursory Research for Embryonic Science and Technology (PRESTO), Japan Science and Technology Agency (JST) (D.J.). D.J. thanks the JSPS Asian core program. H.I. thanks the Creative Research Initiatives (Center for Time-Resolved Diffraction) of MEST/KOSEF for a grant.

Supporting Information Available: Details regarding the synthetic procedure, self-assembly, spectral profiles, and PXRD simulation. This material is available free of charge via the Internet at http://pubs.acs.org.

JA901357H